

# ON THE COUPLING OF ROTATION POWERED PULSARS TO PLERIONIC NEBULAE

JONATHAN ARONS

*Department of Astronomy and Department of Physics  
University of California, Berkeley*

**ABSTRACT.** After discussion of observational constraints on the nature of the MHD wind coupling between the Crab Pulsar and the Crab Nebula, the theory of transverse relativistic shock structure is reviewed and applied to the interpretation of the wisps in the Nebula as the manifestation of the distributed wind termination shock structure, energetically dominated by heavy ions, accelerated in the rotational equator of the pulsar to energies comparable to the total voltage across the pulsar's open field lines and carrying a current comparable to the Goldreich-Julian current. New results on the variability of the shock structure are presented, which show that the gyrating ion bunches emit outwardly traveling finite amplitude compressional waves, in agreement with recent ground based observations. The implications of the theory for X-ray,  $\gamma$ -ray and high energy neutrino emission are briefly discussed, as are the problems of low magnetic energy density in the upstream wind and the origin of the Nebular radio emission. A brief discussion of other plerions leads to the conclusion that much more detailed observations are needed before these systems can be modeled with the same sophistication as can be done for the Crab Nebula.

## 1. Introduction

Pulsars and soft gamma ray repeaters (SGRs), known to be neutron stars with varying levels of confidence, are unresolved stellar sources. Rotation powered pulsars lose most of their energy in an invisible form; SGRs may also lose much of their energy in the same manner. Sometimes, this energy loss leaves its signature in the form of unpulsed nonthermal emission from surrounding nebulae - the positional identification of such nebulae with SGRs is the main argument for identifying the SGR phenomenon with neutron stars (Kulkarni, this meeting). The nebular nonthermal radiation is synchrotron and inverse Compton emission from relativistic particles and fields injected by the embedded pulsar.

The Crab Nebula is the most famous example of a plerion which forms a box calorimeter around its pulsar. Other well known examples include Vela-X (Bock *et al.* 1998) and 3C58 (*e.g.* Helfand *et al.* 1994), although in this latter nebula no pulsar has been specifically identified. There are about 15 plerions identified from radio images, while recent advances in X-ray imaging have found clear evidence for X-ray nebulae (presumably synchrotron nebulae) around pulsars (Harrus *et al.* 1996).

When the pulsar's energy loss is relatively small and the pulsar's space velocity is high, calorimetric nebulae enclosing the pulsar change their morphology and assume a

cometary form. This change occurs when the space velocity of the pulsar exceeds the expansion velocity the plerion would have if the pulsar were stationary with respect to the interstellar medium. If the pulsar's true age equals its characteristic age, then one expects to see cometary morphology or other distortions when

$$t_{char} \equiv \frac{P}{2\dot{P}} > \frac{10^4}{v_{100}^{5/3} P^{2/3}} \left( \frac{I_{45}}{n_{ISM}} \right)^{1/3} \text{ years}; \quad (1)$$

younger objects should be well embedded inside their nebulae. Here the rotation period  $P$  is in seconds,  $I_{45}$  is the moment of inertia measured in units of  $10^{45}$  cgs,  $v_{100}$  is the pulsar's space velocity in units of 100 km/s, and the interstellar particle number density is in units of  $\text{cm}^{-3}$ . A subset of such "plerionic" nebulae forms within binary systems, when the pulsar's outflow energy interacts with either the companion star or with the mass loss from that star (Arons and Tavani 1993).

The calorimetric nebulae surrounding young pulsars are of particular interest, since understanding the physics of nebular excitation in these systems can yield reasonably unambiguous constraints on the physics of the underlying pulsar, without the geometric confusion introduced by the more complex flows around older pulsars. The Crab Nebula is still the only system in which the quality and quantity of observational information enables meaningful physical progress at a fundamental level.

## 2. The Crab Nebula: The Interaction of PSR 0531+21 with the World

This remnant of SN1054 emits nebular radio, IR, optical, X- and  $\gamma$ -rays ( $\varepsilon < 100$  MeV), all of which is synchrotron emission; higher energy photons probably are the Inverse Compton emission of the same electrons (and positrons) that emit the synchrotron radiation (de Jager and Harding 1992). The synchrotron lifetimes of the particles which emit photons at near-IR and shorter wavelengths are less than the age of the nebula, thus requiring a continuous source of power, a requirement fulfilled by the central pulsar, whose spin down luminosity  $\dot{E}_R \approx 5 \times 10^{38}$  ergs/s exceeds the total nebular luminosity (primarily in X-rays and  $\gamma$ -rays) by about an order of magnitude - the pulsar has  $\sim 10\%$  efficiency in converting rotational energy loss into instantaneous particle acceleration power in the Nebula. Furthermore, this power gets delivered to particles whose maximum energy, as judged by the particle energies needed to radiate 100 MeV synchrotron photons, is  $\geq 10^{15.5}$  eV, comparable to the total voltage drop across the pulsar's open field lines. The radiative lifetime of these 3 PeV electrons and positrons is quite short,  $\sim$  months; X-ray emitters lose energy in a few years. Thus the high energy nebular emission provides a window into the pulsar's energetics right now, demanding  $10^{38.5} - 10^{39}$  electrons and positrons per second from the pulsar, assuming the particles are accelerated only once. The shrinkage of the nebular image with increasing photon energy shows that acceleration indeed does occur only once, and must be substantially complete at radii no larger than the X-ray torus seen in ROSAT images, *i.e.*, at projected radii less than 0.3 - 0.6 pc from the pulsar. The gamma ray source may well be smaller than the X-ray torus, as is suggested by the hard X-ray image of Pelling *et al.* (1987). If the acceleration process varies on time scales comparable to or longer than the

radiative lifetime of the  $\gamma$ -rays (for example), then the gamma ray flux from the nebula will vary, since the short lived particles' energy density and emissivity then follows the time variable acceleration physics. EGRET data have suggested that some gamma ray variability does occur on a time scale of months to years (de Jager *et al.* 1996).

By contrast, the radio and far IR emitting particles have synchrotron lifetimes greater than the nebular age. Therefore, their emission depends on the history of the nebula, representing a convolution of the pulsar's efficiency as a provider of accelerated particle energy, particle number and magnetic field with the expansion history of the nonthermal bag. The expansion history depends on the density and geometry of the external medium that confines the relativistic particles and fields. Averaging over the nebula's history, the lower energy particles in the nebula show that the pulsar has provided roughly  $10^{40}$  synchrotron radiating particles/s. The discrepancy between this average injection rate and the instantaneous injection rate to the X-ray torus has not been resolved - the pulsar might have been a substantially more active provider of relativistic particles in earlier epochs, or it might provide an additional source of low energy particles today which is not associated with the X-ray torus. The nonthermal emission requires nonthermal nebular distributions of particles in energy space - "power laws", in the simplest representation of the data.

Images are essential to understanding the physics (radio, optical, UV, X-Ray; hard X-ray and  $\gamma$ -ray if we could get them): for starters, the shrinkage of the nebular image with increasing photon energy shows that the acceleration site is at or near the pulsar, not distributed throughout the nebula, at least for the higher energy particles. Detailed imagery (radio, near IR, visual, soft X-ray) reveals the fine structure of the region where the pulsar rotational energy loss appears to be delivered to the nebula. As has been known since their discovery by Lampland (1921), the NE-SW direction from the pulsar (the short axis of Nebula) shows "wisps", time variable (months to days) surface brightness enhancements which are always present, between 5 and 30 arc seconds from the pulsar (0.05 to 0.3 pc projected radius). If one assumes the nebula to be "optically thick" to the relativistic ram pressure  $\dot{E}_R/4\pi r^2 c$  of the unseen outflow, balancing this ram pressure with the total nebular pressure ( $p_{neb} \sim 10^{-8}$  dynes/cm<sup>2</sup>) yields a termination radius for the unseen outflow right in the middle of the wisp region (Rees and Gunn 1974), thus suggesting very strongly that the wisps are an observational signature of the coupling between the pulsar and the nebula. Recent ground based optical studies have shown these variations appear to be waves in brightness traveling outwards with speed  $\leq 0.5c$  (Tanvir *et al* 1997), a result consistent with the preliminary results of the ongoing HST imaging campaign (J. Hester and J. Graham, personal communications). These variations are not correlated with timing glitches and other rotational noise features of the pulsar, thus suggesting the variability is an intrinsic feature of the mechanism which couples the unseen pulsar energy outflow to the nebula, rather than being a passive consequence of variability in the pulsar's spindown.

The most efficient hypothesis is to assume the wisp region is the particle acceleration zone, in addition to being the region where the pulsar outflow energy becomes coupled to the nebular plasma. In this context "acceleration" means the conversion of the outflow energy, whatever it is, into the spectra of electrons and positrons which are injected into the nebula. As in the acceleration of cosmic rays by supernova remnant

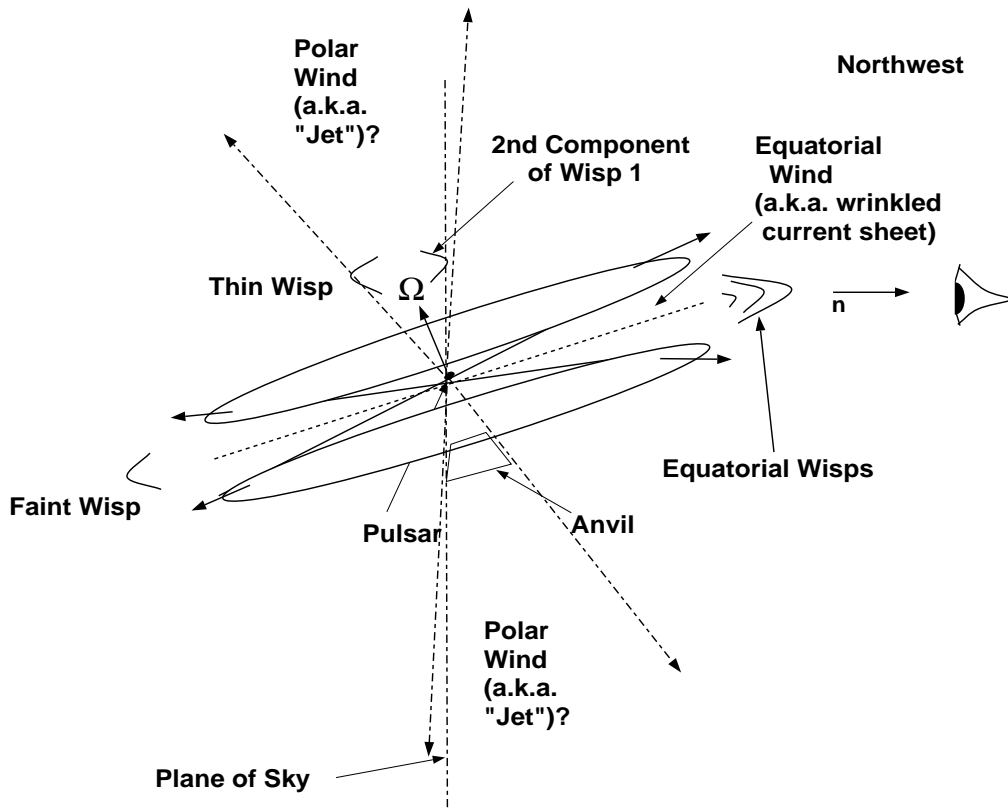


Fig. 1. The outflow geometry around the Crab Pulsar, after Hester *et al.* 1995.

shocks rather than by supernovae themselves, such a hypothesis avoids the problem of the adiabatic losses which plague mechanisms which rely on accelerating the observed particle spectra within the pulsar's magnetosphere (e.g., Tademaru 1973). Granted that the wisp variability time scale is months, that the  $\gamma$ -ray emitting particles have radiative loss times on the same order, and that EGRET may well have seen some gamma ray variability on month to year time scales, I am much attracted by the hypothesis that the variable wisps are the direct signature of the acceleration of particles to gamma ray emitting energies, and thus are the site of the high energy electron and positron acceleration in the Crab Nebula.

### 3. Wind Outflow From Crab Pulsar

Figure 1 shows a cartoon of the flow geometry near the Crab Pulsar. The X-ray morphology implies an outflowing "disk wind" in the equator, possibly associated with a corrugated equatorial return current sheet, which terminates at or within the X-ray torus

- in most interpretations, the termination point identified depends on which feature the interpreter adopts as a termination shock, implicitly assumed to be infinitesimally thin on the scales of observational angular resolution. The polar outflow appears in the HST imagery as arcs both concave and convex toward the pulsar (the thin wisp and the second, time stationary strand of wisp 1), interpreted as possible shocks in a polar “jet” by Hester *et al* (1995). Within the context of the fully MHD wind theories advanced by Kennel and Coroniti (1984a,b), hoop stress in the toroidal magnetic field at high latitude may compress the flow axially, contributing to the polar X-ray enhancements - the bolometric synchrotron surface brightness scales  $\propto B^4$  (Woltjer 1958, Gallant and Arons 1994). If so, the arc features identified by Hester *et al.* might be interpretable as parts of a polar termination shock’s structure, in a manner similar to the theory of the equatorial wind’s termination described below. However, such speculations are for future investigation, and will not be discussed further here.

It seems hard to avoid the conclusion that the outflowing energy feeding the X-ray torus has the character of a relativistic MHD wind. The most widely accepted models of the electrodynamics of pulsars’ polar caps require an electric current along polar field lines with density  $J_{\parallel} \approx B/P$ , which yields a total current  $I_{\parallel} = 2\mu\Omega_*^2/c$  - here  $\Omega_* = 2\pi/P$  and  $\mu$  is the magnetic moment. If the polar current couples to the wind/nebula (an open circuit on light cylinder scales), the current induced  $B$  makes a considerable contribution to pulsar torque, a theoretical possibility supported by the fact that observed torques don’t depend significantly on obliquity (Lyne and Manchester 1988). In such open circuited models, the number of electric current carrying particles shot into the nebula per unit time is  $\dot{N}_R = I_{\parallel}/Ze = 2\mu\Omega_*^2/Zec$ , where  $Z$  is the atomic number of the current carrying particles.  $Z=1$  if the polar current is electrons, as is the case when the obliquity between the magnetic moment and the rotation axis is less than  $90^\circ$ , the geometry believed to be appropriate for the Crab Pulsar (*e.g.* Romani 1996).

Note that such models require another particle outflow from the neutron star to supply the required return current! For open circuited models, this outflow probably is particles of the opposite charge sign extracted from an “auroral ring” around the polar flux tube, *ejected along the field lines that map into the rotational equator of the PSR*, there to flow out in the (corrugated) equatorial current sheet. The return current in open circuited theory is still a cartoon - its dynamics has yet to be explored. The results of shock theory applied to the equatorial wind strongly suggest this return current in the Crab to be heavy ions, accelerated to the full potential drop available (see below).

For the Crab, the number of electrons and positrons required to feed the X-ray source tells us that at least in the equatorial wind, the pulsar’s loss rate in pairs is

$$\dot{N}_{\pm} \sim 10^{38.5-39} \text{ s}^{-1} \gg \dot{N}_R(\text{Crab}) \simeq 10^{34.2} \text{ s}^{-1}. \quad (2)$$

It is well known that in pulsar flows, a total outflow rate of quasi-neutral plasma in excess of  $\dot{N}_R$  is a necessary condition for applicability of relativistic MHD as the underlying theory (Arons 1979). Therefore, the simplest theory for the equatorial outflow is that the spindown energy loss is carried by a relativistic MHD wind, with electrons and positrons as the main constituents by number. This wind might also contain a minority population of heavy ions, which may or may not be energetically significant, and may

also carry part of the energy flow in the Poynting flux of the wound up electromagnetic fields.

The rotational energy lost in nonradiative fields, pairs, heavy ions carried by a MHD wind through the radiationless cavity at  $r < 0.1$  pc from the pulsar has its energy conservation described by

$$\begin{aligned}\dot{E}_R &= r^2 \int d\Omega \left\{ \frac{c}{4\pi} \mathbf{E} \times \mathbf{B} + \mathbf{v}_{wind} \gamma_{wind} [(n_+ + n_-) m_{\pm} c^2 + n_i m_i c^2] \right\} \cdot \hat{\mathbf{r}} \\ &= c \beta_{wind} \gamma_{wind} \dot{N}_i m_i c^2 \left( 1 + \frac{m_{\pm}}{m_i} \frac{n_+ + n_-}{n_i} \right) (1 + \sigma),\end{aligned}\quad (3)$$

with the solid angle integration carried out over the sector of interest - an equatorial sector with total latitudinal opening angle on the order of  $20^\circ$ , if the wind feeding the observed X-ray torus has straight streamlines. The parameters

- $m_i \dot{N}_i$  = mass loss rate in ions
- $(n_+ + n_-)/n_i = \dot{N}_{\pm}/\dot{N}_i$  = ratio of pair number loss rate to ion number loss rate
- $\gamma_1$  = the bulk flow Lorentz factor (or the velocity  $v_1$ )
- $\sigma$  = ratio of Poynting flux to kinetic energy flux in the wind

characterize the wind's properties.

MHD wind theory with  $\sigma \ll 1$  gives a “natural” explanation of the Crab Nebula's dynamics<sup>1</sup> (Rees and Gunn 1974, Kennel and Coroniti 1984):

- The deceleration of the post shock, low  $\sigma$  pulsar wind ( $v_r \propto 1/r^2$ ) compresses the magnetic field ( $B \propto r$ ) until the magnetic energy reaches equipartition with the shocked relativistic plasma energy, whence deceleration and compression ceases - the model neatly explains equipartition as a dynamical effect;
- The fit to the observed expansion velocity requires  $\sigma \ll 1$  (caveat - Kennel and Coroniti neglected possible inertial loading by the filaments);
- If the wind termination shock is assumed to create power law distributions of pairs, with upper and lower cutoffs determined by the jump conditions and the particle spectral index at the shock constrained by the final fit to the data, the global optical, X- and

---

<sup>1</sup> Recently Begelman (1998) proposed that MHD kink instability of toroidal magnetic fields allows one to construct a wind fed model of the Crab with  $\sigma \sim 1$  in the wind, a conclusion which depends on the assumption, unstated in his paper, that the kinked magnetic fields coagulate into patches whose filling factor in the nebula is small, and within which most of the field energy annihilates. Such coagulation is not a known consequence of the kink instability (quite well studied in the low  $\beta$  plasmas in fusion devices and the solar corona), and the virial theorem suggests such coagulation to be unlikely. The observed uniformity of the radio spectral index (Bietenholtz and Kronberg 1992) shows that the proposed annihilation must have little radiative consequences for the radio emission in the Nebula, which is energetically surprising. If a kink instability does occur, a more likely consequence of kinking and reconnection would be to fill the Nebula with magnetic loops whose filling factor is on the order of unity, in which case Rees and Gunn's original arguments for low  $\sigma$  in the wind are unaltered. Nevertheless, the fine fibered structure observed by Scargle (1969) and by Hester *et al.* (1995) in the optical emission from the Nebula suggests some mechanism for complicating the magnetic structure on a fine scale is at work, for which Begelman's kink instability is a candidate.

gamma-ray spectrum of the Crab can be reproduced by the model, once synchrotron cooling in the flow is properly incorporated (Kennel and Coroniti 1984b).

But, radio emission from the Nebula is entirely left out! The inferred particle injection rate (*now*, since rapid synchrotron losses make the X-rays a calorimeter for the current injection rate) is an order of magnitude smaller than the rate of injection of radio emitting particles, averaged over the life of the Nebula. Thus, the main stored component of the relativistic energy in the Nebula was neglected. The non-spherical morphology was not quantitatively addressed. Conceivably, the problem of radio emitting particle injection is related to the strong latitudinal asymmetries revealed by HST and other imaging.

#### 4. Physics of Relativistic Shock Structure/Dissipation/Acceleration

As remarked above, dynamic pressure balance puts the termination of the pulsar's unseen outflow at  $r_s \sim 0.1 - 0.2$  pc (Rees and Gunn 1974). Shock dissipation is the most likely wind termination mechanism in the MHD theory. A shock in a MHD outflow from the Crab pulsar must be transverse:  $\angle(\mathbf{B}, \mathbf{v}) \approx \pi/2 - 10^{-9} \Rightarrow$  diffusive Fermi acceleration has little relevance to the conversion of flow energy into power law distributions of particles downstream. The phenomenological shock model with the shock regarded as infinitesimally thin and located at  $r_s \approx r_{\text{wisp}}$  simply requires the conversion of  $\sim 10\%$  of the flow energy into the spectra of pairs with distribution functions immediately downstream of the shock  $N_{\text{injected}}(\gamma) \propto \gamma^{-s}$ ,  $s \approx 2.2$ ; it doesn't explain how the system achieves this efficiency.

My contributions to the subject come partly under this heading. The results, based on linear instability theory, particle-in-cell simulations and a modicum of quasi-linear theory, were mostly published some time ago (Alsop and Arons 1988, Langdon *et al.* 1988, Hoshino and Arons 1991, Gallant *et al.* 1992, Hoshino *et al.* 1992). Those interested in the detailed support of most of the assertions made in this section should consult the papers referenced.

Imagine what happens when the incoming flow "collides" with the magnetic step formed by the shock. The particles *all* reflect coherently, and start gyrating coherently within the shock front, now considered more realistically as a transition region of finite thickness in the flow. The coherently gyrating particles radiate collective cyclotron and synchrotron waves with fundamental frequencies  $\omega_1 = eB/mc\gamma_1$ , as well as large amounts of power at the harmonics  $\omega_l = l\omega_1$ , including the high harmonics  $l \gg 1$ . The basic mechanism is azimuthal bunching of the ring distributions in momentum space set up by the coherent reflection from the magnetic step, whose shape is self-consistently maintained by the particle rings in momentum space. The pairs radiate extraordinary modes, with  $\omega_1 \geq (eB_1/m_{\pm}c\gamma_1)\sigma^{-1/2} \sim 10^{-3} \text{ s}^{-1}$ . The numerical value assumes the upstream magnetic field to be  $B_1 \sim 10^{-4.5}$  Gauss, the upstream flow Lorentz factor to be  $\gamma_1 \sim 10^6$  and  $\sigma \sim 10^{-2.5}$ , all values taken from the Kennel and Coroniti model or from the Gallant and Arons (1994) model described below. Coherent gyration of heavy ions as they encounter the magnetic step excites transverse magnetosonic waves which propagate with properties mainly determined by the pairs (if the pairs are numerically in the majority, as turns out to be the case), with frequencies  $\omega \geq ZeB_1/m_i c\gamma_1 \sim 10^{-6.5} \text{ s}^{-1}$ ,

a gyration time of months<sup>2</sup>.

Cyclotron reabsorption of the extraordinary modes at the shock's leading edge thermalizes the pairs to a relativistic Maxwellian distribution with downstream temperature  $T_{\pm} \approx \gamma_1 m_{\pm} c^2$  - the mean free path for extraordinary mode emission and absorption in the pair plasma is much smaller than the flow scale length, leading to the establishment of local thermodynamic equilibrium for essentially the same reason that the emission and absorption of virtual photons (Coulomb collisions) establishes LTE in a collisional nonrelativistic plasma - in the relativistic case, the pairs and their waves form a local *hohlraum*. The relativistic cyclotron instability in the ions simply serves to establish a level of electromagnetic fluctuations (corresponding to real photons in this case) at the thermal level far faster than would occur if two body encounters were the only means of creating the fluctuating electromagnetic field. The simulations show that when pair thermalization is complete, the radiation level also corresponds to LTE (in the Rayleigh-Jeans limit, as is expected for these classical investigations).

From the perspective of the pairs, the magnetosonic waves emitted by the more slowly developing relativistic ion cyclotron instability are an external source of energy, which can upset their thermal equilibrium. The simulations show that the magnetosonic waves have a nonthermal spectrum, basically corresponding to  $1/f$  noise. These waves are preferentially cyclotron absorbed by the more mobile pairs, first at ion harmonics  $l \sim m_i/Zm_{\pm}$ , then, as the pairs gain energy and detune from the high harmonics, from waves in the power law spectrum with successively lower frequencies, until acceleration stops for pairs whose energy equals that of an upstream ion, for which the cyclotron frequency equals that of the ions that drive the acceleration.

Indeed, a simple application of quasi-linear theory to this process (Arons, unpublished) shows that the acceleration rate of an electron or a positron in a spectrum of linearly polarized magnetosonic waves

$$U_k = r_{Li} \frac{(\delta B)^2}{4\pi} (kr_{Li})^{-2}, \quad (4)$$

the spectrum exhibited by the simulations, is

$$\frac{\dot{\gamma}}{\gamma} = \frac{0.017}{n_0^3} \left( \frac{\delta B}{B} \right)^2 \Omega_{Li}. \quad (5)$$

Here  $k$  is the wavenumber,  $U_k dk$  is the wave energy density in the interval  $(k, k + dk)$ ,  $r_{Li} = c/\Omega_{Li}$  is an ion's Larmor radius and  $\Omega_{Li}$  its relativistic Larmor frequency, and

$$n_0 = \left( \frac{c^2 + v_A^2}{c_s^2 + v_A^2} \right)^{1/2}, \quad (6)$$

is the index of refraction of low frequency, small amplitude magnetosonic waves in the pairs, with  $c_s$  the relativistic sound speed in the pairs and  $v_A$  the relativistic Alfvén

---

<sup>2</sup> In the actual application to the Crab, the ions gyrate in a  $B$  field already compressed by a factor of two to three above its upstream value by the preliminary shock in the pairs, which increases the gyration frequency by the same factor and yields an ion gyration time of 1-2 months.

speed in the relativistically hot pairs. Typically  $n_0 \sim \sqrt{2} - \sqrt{3}$ . Formal applicability of quasi-linear theory requires  $\delta B/B \ll 1$ , while the simulations show that  $\delta B/B > 2$  for parameters of interest. Nevertheless, the simulations show that the acceleration rate is indeed Fermi-like, with  $\dot{\gamma}/\gamma \sim \Omega_{Li}$  - quasi-linear theory yields the correct scaling of the rate for the resonant process even when the fluctuation amplitudes are large, although its estimate of the numerical value is less reliable.

Subjected to the nonthermal heating of this resonant absorption process, with losses being simply outflow of pairs from the region where the ions lose their energy to the pairs, the relativistic Maxwellian pairs downstream from the pair shock develop a nonthermal distribution

$$N_{\pm}(\gamma) \propto \gamma^{-2}, \quad \gamma_1 < \gamma < (m_i/Zm_{\pm})\gamma_1. \quad (7)$$

For lower energies, the particle spectrum remains that of a relativistic Maxwellian. The efficiency of energy transfer from the ions to the pairs is

$$\varepsilon_a = \frac{\text{nonthermal pair energy}}{\text{total upstream flow energy}} \approx 10 - 20\%, \quad (8)$$

a result known solely from simulation. These acceleration results obtain when the ions provide the largest component of the upstream flow energy, and are remarkably like those inferred from application of ideal MHD shock theory to the Crab Nebula, with power law populations of pairs assumed in the post shock flow.

## 5. Wisps as Internal Shock Structure

The physics of these shocks implies a model for the coupling of the equatorial wind outflow from the Crab pulsar. Suppose the equatorial flow to be composed of  $e^{\pm}$  pairs, heavy ions and wound up magnetic fields in an unknown mixture, all flowing out from the pulsar at super-Alfvénic speed. The shock thermalizes the pairs to a relativistic Maxwellian distribution within the leading edge of the shock structure - this thermalization region has radial thickness  $\sim r_{L\pm} \sim 10$  AU, unobservably thin to all but VLBI radio observations. The ions have much larger gyration radius in the compressed magnetic field supported by the shock heated pairs ( $r_{Li} \sim 0.3 A/Z$  pc). Relativistic cyclotron instability of the gyrating ions generates large amplitude, long wavelength ( $\lambda \sim 0.2/l$  pc,  $l \geq 1$ ), *compressional*, linearly polarized magnetosonic waves in the heated pairs. Cyclotron absorption of these waves causes gradual nonthermal acceleration of the pairs over a length  $\sim$  several ion Larmor radii<sup>3</sup>. The ions follow a coherent orbit for a couple of gyration cycles, becoming progressively more disorganized as the instability broadens their momentum distribution and drains their energy into magnetosonic waves. However, in the first few cycles of coherent gyration flow, the turning points in the ion orbits are coherently spaced with separations  $\sim r_{Li}$ . Since the radial outflow (and inflow) momentum of the gyrating ions must be deposited in the magnetized pairs as the ions gyrate, the

---

<sup>3</sup> This length is the distance required to bring the highest energy pairs in the spectrum to their maximum energy  $\sim \gamma_1 m_i c^2$ , at which energy they radiate 100 MeV gamma rays. The nonthermal spectrum of infrared and optically emitting particles is established within a distance  $\sim 10r_{L\pm} \approx 100$  AU downstream of the leading edge shock in the pairs. Therefore, one needs better than 10 mas angular resolution to allow detection of the initially thermal O/IR synchrotron spectrum.

turning points correspond to compressions in the magnetic field and pair plasma. Such compressions correspond to surface brightness enhancements separated in radius by the ion Larmor radius scale, with bolometric synchrotron emissivity  $\propto B^4$ . The compressions also couple the ion momentum to the propagating magnetosonic waves of the pair plasma, since the cyclotron instability makes the ion reflection process time dependent in the ion drift frame. Thus the compressions created by the reflected ions should travel outwards in the pair flow frame with the magnetosonic speed of the nonlinear waves.

The properties of such compressions have a not unreasonable similarity to the observed properties of the wisps, suggesting that the wisps are the observable manifestation of the *internal structure* of an (energetically) ion dominated shock terminating the equatorial wind from the Crab pulsar. If this hypothesis is correct, the whole shock structure is spread across the sky, turning the Crab Nebula into a laboratory for the relativistic shock physics believed to be central to a wide variety of high energy astrophysical systems.

Gallant and Arons (1994) decided to test the configuration space aspects of the model outlined above by constructing a quantitative *steady* flow theory, assuming the flow to be confined to a sector of a sphere within latitude  $\sim \pm 10^\circ$  of the pulsar's rotational equator. The ion flow was modeled as a *laminar* stream of particles with no momentum dispersion, gyrating in the magnetic field embedded in a shock heated, Maxwellian pair fluid whose flow was modeled as adiabatic - no attempt was made to model either the nonthermal particle acceleration or the variability observed in the simulations, and by construction the model creates compressions which are stationary in space - the pairs flow through these standing waves. This model and its quantitative results, when applied to the I-band snapshot of van den Bergh and Pritchett (1988), are illustrated in Figure 2.

Among the model's highlights are a simple explanation of the NW-SE brightness asymmetry of the wisps as being due to the Doppler boost in the mildly relativistic pair flow in the ion gyration region. The parameters inferred from the best fit of the model to the main wisps 1 and 2 in the NW and the faint wisp in the SE suggest this steady, reflected ion flow model has not unreasonable correspondence to van den Bergh and Pritchett's observations of wisp separation, brightness and shape, which overdetermine the model:

$$\begin{aligned} \sigma &\approx 3 \times 10^{-3}, \\ \gamma_1 &\approx 4 \times 10^6 \approx 0.3Ze\Phi_{open}/m_i c^2, \\ B_1 &\approx 3 \times 10^{-5} \text{ Gauss}, \\ \dot{N}_\pm &\approx 10^{38} \text{ s}^{-1}, \\ m_i \dot{N}_i &\approx 2m_\pm \dot{N}_\pm \approx 10^{-15} M_\odot/\text{yr} \approx 50,000 \text{ metric tons/s}, \\ Z\dot{N}_i &\approx 3 \times 10^{34} \text{ s}^{-1} \approx \text{Goldreich - Julian return current}. \end{aligned}$$

Here  $\Phi_{open} = \sqrt{\dot{E}_R/c} = 4 \times 10^{16}$  Volts is the total electric potential drop across the open magnetosphere. The fit to the data also fixes the ion Larmor radius and the tip angle of the equatorial outflow to the line of sight:  $r_{Li} \approx 0.15$  pc and  $\angle(\text{LOS}, \text{equatorial wind}) \approx 35^\circ$ . The number of pairs flowing out in the equatorial wind is close to, but somewhat less than what was inferred in the Kennel and Coroniti model as the particle

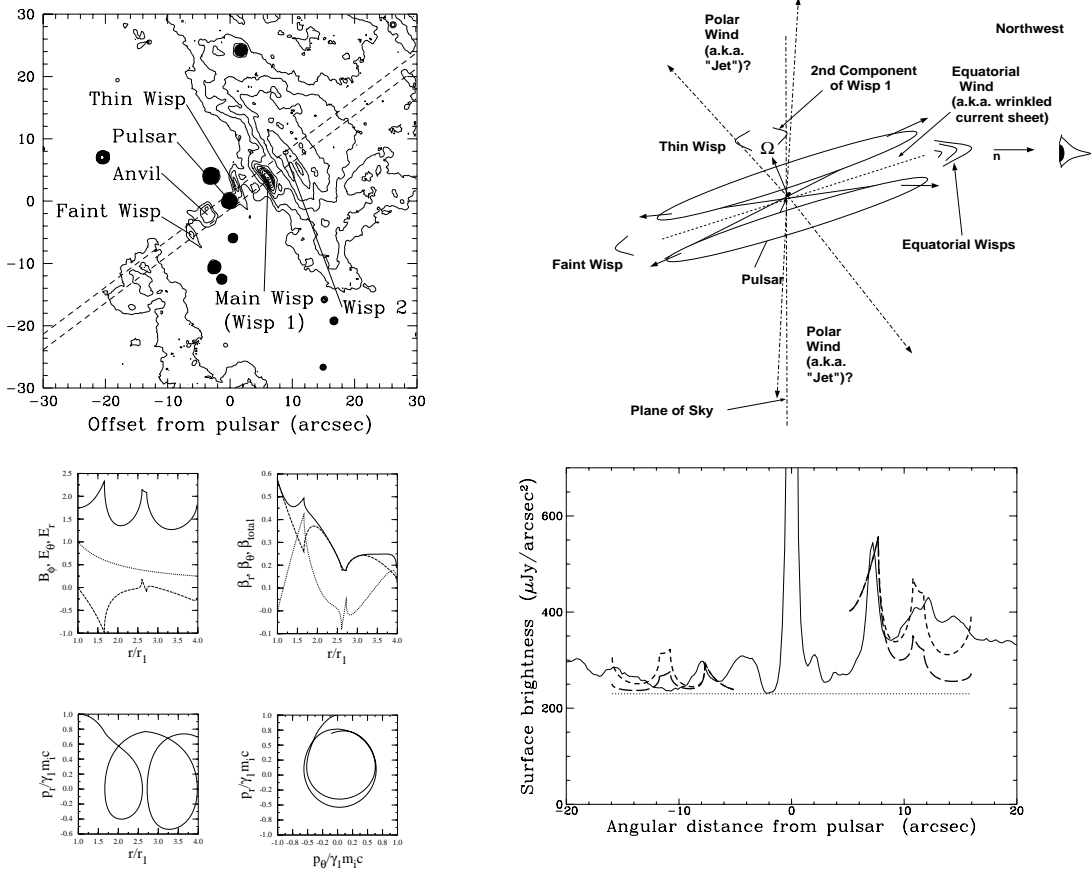


Fig. 2. The Gallant and Arons (1994) model. Upper left panel: The van den Bergh and Pritchett 1989 image of the Crab's central regions. The surface brightness in the strip between the dashed lines was used to provide the data with which the model is compared. Upper right panel: The geometry of the region around the pulsar, as in Figure 1. Lower left panel: The theoretical structure of the model - upper left: B field (top curve), transverse E field (middle curve), radial E field (bottom curve); upper right: flow velocity of the pairs (top = total, middle = radial, bottom = transverse current velocity); lower left: radial ion momentum as a function of position; lower right: ion phase space, showing the laminar ring orbits. Lower right panel: synthetic surface brightness compared to the observations: dashed curve with large central peak - the I-band data from van den Bergh and Pritchett (1989); remaining dashed curves - the models, assuming thermal synchrotron emission from the pairs, for two different assumptions about the rate of pitch angle broadening of the anisotropic pair distributions. Note the failure of the model to account for the thin wisp, for the bifurcated structure of wisp 1 and for the anvil, failures which are all a consequence of the fact that these extra features are due to superposition of features in the polar flow on the images of the equatorial structures when projected onto the plane of the sky.

supply needed for the X-ray source, and the ion current is in good agreement with what one would expect if the equatorial wind carries the return current.

While the favorable comparison of the Gallant and Arons model to a single, relatively low resolution optical snapshot of the Crab gives some credence to the basic idea that the wind is energetically dominated by very high rigidity ions, the neglect of time dependence is a serious flaw in modeling the equatorial outflow. Variability of the equatorial wisps has been known since Lampland’s original discovery, seen most spectacularly in the high resolution “movie” created from the HST campaign now in progress and in the ground based optical observations reported by Tanvir *et al.* (1997). Both sets of data show that the wisps are outwardly propagating structures, behaving like spherical or cylindrical waves which lose coherence over several tenths of a parsec as they propagate away from the pulsar.

The kinetic simulations of ion dominated relativistic shocks in plane parallel geometry published by Hoshino *et al.* (1992) (see also Hoshino 1998) clearly show the shock structure to be time dependent, with a large amount of short wavelength power in the magnetic field. The basic relativistic cyclotron instability of the shock structure implies variability of brightness enhancements on the ion gyration time scale, with faster variability imposed on the basic structure by the higher harmonics. Such variability would be uncorrelated with pulsar timing variations, as seems to be the case in all the observations of wisp variability. However, the original simulations did not give a clear answer to whether the variability is in the form of oscillations of the shock structure around a mean position, or in the form of “radiation” of finite amplitude magnetosonic waves into the surrounding nebula.

An investigation of the time dependent theory (Spitkovsky and Arons, in prep) shows that the relativistic cyclotron instability of the ion ring formed immediately downstream of the thin shock in the pairs *does* launch outwardly running waves in the magnetic field, density and temperature of the pairs (contrary to the criticism of this model advanced by Tanvir *et al.* 1997, who assumed that shock variability corresponds to shock oscillation around a mean position), with fundamental period comparable to the ion Larmor time  $t_{Li} = 2\pi c/\Omega_{ci2} = m_i c \gamma_1 / Ze(3B_2) \approx 1.5$  months.

These calculations use a “hybrid” approach to modeling the shock structure. Particle-in-cell ions are injected into hot (Maxwellian) pairs, modeled as an ideal, relativistic MHD fluid with magnetic field transverse to the flow. The pair fluid is still modeled as adiabatic, with cyclotron absorption of the ion waves and nonthermal pair acceleration neglected. Some illustrative results from a plane parallel simulation are shown in Figure 3, which shows the compressions in the  $B$  field that form as the ion ring breaks down into time dependent bunches in gyrophase. The compressions in the pairs and  $B$  field observed in the code travel downstream with speed  $v_{\text{wave}} \approx 0.8c$ ; theoretically, small amplitude waves should travel with speed<sup>4</sup>

$$v_{\text{wave}} = \frac{v_{\text{pairs}} + v_{\text{ms}}}{1 + \frac{v_{\text{pairs}} v_{\text{ms}}}{c^2}} = \frac{\frac{c}{3} + \frac{c}{\sqrt{2}}}{1 + \frac{\frac{c}{3} \frac{c}{\sqrt{2}}}{c^2}} = 0.84c.$$

---

<sup>4</sup> The adiabatic index of the pair fluid used in the simulation was  $\Gamma = 3/2$ , as would be the case if the pairs were heated only in the plane orthogonal to  $\mathbf{B}$ .

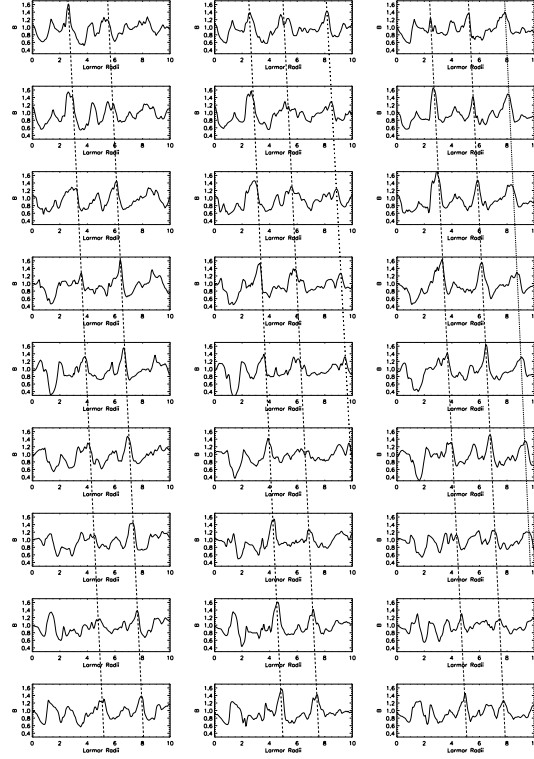


Fig. 3. Snapshots of the magnetic field as a function of position, from a plane-parallel hybrid simulation of the relativistic cyclotron instability of an ion beam injected into a relativistically hot  $e^\pm$  magnetized plasma itself moving with speed  $v_x = c/3$ , with the  $B$  field transverse to the flow. The snapshots are read starting from the top of the left column, then continuing to the second and third columns. The time between each snapshot is  $t_{Li}/18$ . The sloping lines connect identifiable features in the wave profile, which themselves vary in the frame traveling with the wave group velocity. The slopes of these lines provide the wave speed in the simulation frame.

Here  $v_{ms}$  is the wave group speed in the proper frame of the pair fluid. The numerical value is peculiar to the plane parallel geometry used in this particular calculation (mainly to test the code). These preliminary results suggest that the interpretation of the wisp region as the equatorial shock structure remains viable.

## 6. Speculations and Conclusions

These dynamic models of distributed shock structure continue to show promise in the interpretation of the energy transfer between the Crab pulsar and its nebula. A complete theory requires addressing a variety of other issues, which one can only do at the order of magnitude level at present.

## 6.1. X-rays and Gamma Rays

The plane parallel shock structure and acceleration calculations, and quasi-linear theory applied to those simulations, yield the maximum energy of the power law formed in the downstream pairs to be  $E_{\pm,max} \approx (E_{ion})_{upstream} \approx 0.3Ze\Phi_{open} \approx 10^{16}$  eV. The same calculations yield an acceleration time to extend the power law to the maximum energy to be  $t_a(E_{\pm,max}) \approx \Omega_{Li2}^{-1} \approx 1.5$  months. The resulting synchrotron spectrum rolls off above the photon energy  $\varepsilon_2 \approx 0.3(\hbar e B_2/m_{\pm}c)(m_i/Zm_{\pm})^2\gamma_1^2 \approx 20$  Mev, using the Gallant and Arons parameters, a value quite close to the rolloff energy of the variable  $\gamma$  ray component of the spectrum reported by de Jager *et al.* (1996). The synchrotron loss time at these highest energies is  $t_s(E_{\pm,max}) \sim 4$  months, and the size of the synchrotron source in the 10-100 MeV region then should be  $R_s \leq v_{pairs}t_s \simeq 2 \times 10^{17}$  cm. Furthermore, the spatially progressive nature of the particle acceleration suggests that the size of the source at the highest energies will stop shrinking on scales smaller than about  $10''$ , and that interior to several arc seconds from the pulsar, the higher energy emission should show a “hole” in the surface brightness, with the hole size *decreasing* with decreasing photon energy, until the leading edge shock in the pairs is reached.

Because the shock structure is unsteady, the particle acceleration also varies. When the synchrotron loss time greatly exceeds the variability time scale of the accelerator introduced by the large amplitude magnetosonic waves, the radiation physics averages over the variable particle acceleration. At the highest photon energies, however, the synchrotron loss time is comparable to the fundamental magnetosonic wave time scale, suggesting that the 50-100 MeV synchrotron source varies with fractional luminosity changes

$$\frac{\delta L_{\gamma,synch}}{L_{\gamma,synch}} \approx \frac{t_a(E_{\pm,max})}{t_s(E_{\pm,max})} \approx 0.4.$$

At these photon energies, the inverse Compton source overlaps the synchrotron source in energy space. Since the inverse Compton source must have size comparable to the optical Nebula (de Jager and Harding 1992), there will not be variations of the inverse Compton radiation on these short time scales, with the result that the total 50-100 MeV emission will vary less than the synchrotron component alone. Nevertheless, these predicted variations on the several month time scale should be marginally observable in the EGRET data. Also, a substantial, improvement of angular resolution in hard X-rays will soon allow new probes of the Crab’s inner workings, when the HESSI satellite with its  $2''$  imaging at several hundred keV is launched.

## 6.2. The Radio Nebula

Optical, X- and  $\gamma$ -ray emission diagnoses the coupling physics “today”. The radio emission measures the integral of the pulsar’s input over history - most of the stored relativistic energy is in  $B$  fields and radio emitting particles ( $\sim 10^{50}$  ergs). Averaged over the whole Nebula, the radio emitting spectrum has the form  $N_{\pm}(\gamma) \propto \gamma^{-1.5}$ ,  $10^{2.5} < \gamma < 10^4$ ; indeed, detailed spectral index maps (Bietenholz and Kronberg 1992) show this particle distribution to be remarkably homogeneous.

The wind termination shock models constructed to explain the equatorial wind (Kennel and Coroniti 1984a,b, Gallant and Arons 1994) don't yield  $\overline{N(\gamma)} \propto \gamma^{-s}$ ,  $s \sim 1.5$  at energies small compared to  $10^6 m_{\pm} c^2$ . Also, the pair injection rate inferred in the equatorial wind is between a few and 10 per cent of the average injection rate needed to explain the radio Nebula.

This discrepancy poses the following conundrum. Spectral continuity suggests one mechanism accelerates the synchrotron emitting particles, yet the shock jump conditions applied to the equatorial wind clearly show the particle spectrum must be “cut off” below  $10^6 m_{\pm} c^2$  (Kennel and Coroniti 1984b); in the kinetic theory of the shock acceleration physics, the particle spectrum remains Maxwellian below  $\gamma_1 m_{\pm} c^2$  (Hoshino *et al.* 1992), which yields the same low frequency emissivity as does a sharply cut off distribution,  $f_{\nu} \propto \nu^{1/3}$ , not the observed  $f_{\nu} \propto \nu^{-0.25}$ . It is possible that additional acceleration physics within the shock structure beyond cyclotron resonant absorption of the magnetosonic waves can lead to a nonthermal low energy spectrum like that observed - magnetic pumping is an interesting candidate. But, modifications of the acceleration physics will not alleviate the discrepancy between the rate of pair injection into the equatorial torus and the average injection rate of radio emitting electrons.

The discovery of the “polar jet” (Hester *et al.* 1995) suggests that wind outflow at latitudes  $|\lambda| > 10^\circ$ , which could fill most of the solid angle around the pulsar, might provide the source of the larger number of particles feeding the radio source. If the acceleration physics is the same, perhaps spectral continuity is not a surprise. However, one would be quite surprised to find the wind outside of the magnetic equator to contain an energetically dominant component of heavy ions, for the electrodynamic reasons described earlier. Since the energetic dominance of the ions is essential to the cyclotron resonance acceleration explanation of the nonthermal pairs in the equatorial flow, invoking the same acceleration physics at higher latitudes doesn't look to me to be the right theoretical path. One is left with the possibility that the higher latitude acceleration physics is different, or that radio electrons are accelerated in the outer Nebula (for example, by Fermi I acceleration at the shock just outside the synchrotron Nebula, whose presence was inferred by Sankrit and Hester 1996), and that spectral continuity is just a coincidence. Observations of the spectra of other plerions with sufficient spectral coverage (radio, IR, optical, X-rays) would greatly help in directing the course of theory - if most plerions show substantial spectral discontinuities between radio and higher frequencies, then the Crab's spectral continuity clearly would be coincidental. But if the spectra all show continuity similar to the Crab's, then a solution must be sought in terms of a more unified injection/acceleration scheme than is implied by current theory.

### 6.3. High Energy Neutrinos from the Crab Nebula

In principle, observation of high energy neutrinos from the Crab would be a direct test of the ion doped wind model (and of other ideas concerning ultra high energy ion acceleration by the pulsar, such as the outer gap construction of Bednarek and Protheroe 1997). The following numerical example illustrates the possibilities.

Suppose the pulsar injects heavy ions at the Goldreich and Julian rate,  $\dot{N}_i = 10^{34.5}/Z \text{ s}^{-1}$ , each with energy  $\gamma_i m_i c^2 = \eta Z e \Phi_{open} = 4 \times 10^{16} Z \eta \text{ eV}$ . The ions' Larmor

radii in the nebula are  $r_{Li} = \gamma_i m_i c^2 / Ze B_{neb} = \eta \Phi_{open} / B_{neb} \approx 0.15 \eta (10^{-4} \text{ Gauss} / B_{neb})$  pc. The ions drift out of the Nebula with drift velocity across  $B \sim cr_{Li} / R_{neb} \sim 0.1c$ , a speed about 10 times the hydrodynamic expansion velocity of the nebula. Then the number of ions contained in the Nebula is  $N_i = \dot{N}_i (R_{neb}/c) (R_{neb}/r_{Li}) \sim 6 \times 10^{43} Z^{-1}$ . With a cross section for  $\pi^\pm$  production on the order of 10 mb, and with  $\sim 1 M_\odot$  of thermal material within the nebula (contained in the emission line filaments, corresponding to an average gas density of a few protons/cc), the high energy neutrino luminosity of the Crab Nebula should be at least  $10^{29}$  high energy neutrinos/s. This is a lower limit, since the heavy ions continue to interact with the invisible gas confining the visible synchrotron nebula as they to wander outwards through the unknown magnetic field in the inertially confining material. At 2 kpc distance, the neutrino flux from the Crab should be about  $5 \times 10^{-15}$  neutrinos/cm<sup>2</sup>-s, substantially above background at the  $\sim 10^{16}$  ev energy suggested by this elementary monoenergetic model. At these high energies, the count rate expected in the proposed high energy neutrino observatories is rather low. However, the use of the Crab Nebula as an ion calorimeter through the dynamics of the wisps does not tell us anything about the downstream spectrum of injected ions, and theory of ion acceleration at the pulsar is too primitive to be of much help. If the ions have a sufficiently steep injection spectrum, the production rate of lower energy neutrinos might be much higher.

#### 6.4. Why is $\sigma \ll 1$ ?

One of the most surprising conclusions of the Rees and Gunn (1974) model of the Crab is that  $\sigma \ll 1$  in the wind upstream of the termination shock, a result which has persisted in all of this model's descendents. Since the pulsar's magnetosphere is magnetically dominated ( $\sigma \gg 1$ ), and  $\sigma$  is conserved in simple ideal MHD wind models, the fate of the pulsar's magnetic energy has attracted quite a bit of theoretical attention. Suggestions which appear to have some possibility of success include dissipation of the magnetic field in a striped MHD wind by tearing modes (Coroniti 1990); dissipation of the magnetic field in a striped MHD wind because of insufficient current carriers to support the stripes (Michel 1994); and conversion of MHD flow to dissipative "vacuum" waves in the wind zone (Melatos and Melrose 1996). All of these ideas depend upon most of the magnetic field in the wind having a wave-like structure, either as standing oscillations in the fluid frame (Coroniti, Michel), or as large amplitude waves which propagate with respect to the plasma in the fluid frame, with structure dominated by displacement current even though the waves are subluminal (see also Melatos' paper in these proceedings). If any of these thoughts is on the right track, the low  $\sigma$  problem requires giving up the applied mathematical pleasures of studying the aligned rotator and axisymmetric ideal MHD winds - indeed, one has to give up ideal MHD! None of the proposed ideas, however, has been developed to the point of usefully confronting theory with the elaborate HST pictures or other high resolution observations.

## 6.5. Other Models of the Wisps and the Pulsar-Nebula Coupling

I would be remiss if I neglected discussing some of the other ideas around for the interpretation of the Crab's wisps and what they have to tell us about the pulsar-nebula connection. Woltjer (1958) is the first to suggest the idea that the wisps might be damped magnetosonic waves, perhaps driven by Baade's star, the then mysterious object suspected of having something to do with the energization of the Crab Nebula. Scargle (1969) and Barnes and Scargle (1973) rediscovered this idea, and proposed the wisps to be magnetosonic waves in a relativistic electron-heavy ion plasma, launched by upstream variations of the vacuum magnetic dipole radiation then thought to carry the pulsar's spin down energy. They attributed the time variability of the magnetic dipole radiation timing glitches, not to intrinsic instability in the termination of the strong wave, while the nebular relativistic electron spectrum was attributed to Landau damping ("Barnes damping") of the waves in the Nebular plasma. Unfortunately, the wisp variability does not correlate with glitches, and Barnes damping does not lead to the observed particle spectrum. Nevertheless, the ideas expressed by these authors have a clear relationship to the model I outlined above.

Hester *et al.* (1995, and personal communications), has expressed the opinion that the wisps are thermal instabilities in the post-shock outflow from the pulsar, with the shock itself either unobserved or attributed to one or another of the time variable features seen in the HST pictures. In this case, the observed outflow velocity of the wisp features is the fluid flow speed. The main flaw in this view is that within the Kennel and Coroniti model, from which the suggestion derives, the cooling time is too long ( $\sim 10$  years) for the particles which mainly contribute to the pressure, much longer than the weeks to months needed to explain the variations. Chedia *et al* (1997) suppose the wisps to be drift waves in a low energy pair plasma (whose provenance is not otherwise explained), excited by a  $\gamma \sim 10^6$  ion beam from the pulsar - these authors assume no shock forms, which is contrary to the known dynamics of a relativistic ion beam in the magnetized plasma. Begelman (1998b) hypothesizes the wisps to be travelling surface waves excited by the interaction between an axisymmetric equatorial outflow and a higher latitude outflow traveling with a different four velocity, a model which is not very specific about observational consequences that could discriminate it from other ideas. Presumably still more suggestions will be forthcoming as the quality of the observations continues to improve.

## 7. Other Plerions

One may well ask whether other filled image SNR ("plerions", composite SNR) have the same physics. Unfortunately, none of them have been sufficiently well studied to bring the kind of physical modeling described here to bear. We saw at this meeting the striking advances in X-ray detections of plerions, which, when coupled with existing and new radio observations, allow us to begin asking simple physical questions, such as whether spectral "breaks" between radio and X-ray observations tell us anything about the age of the system, assuming a single mechanism injects a single power law distribution at all energies into the plerion. But until the optical and IR spectral regions are filled in, until

detections are made at energies high enough to allow one to follow possible variability of the acceleration mechanism, and until high angular resolution imaging allows one to study the variable features associated with the acceleration physics, one will be left with only the wonderful example of the Crab as the test of physical theories of pulsars as particle accelerators. The chance that this system's physics does not typify all the pulsar-plerion pairs known or to be found, and by extension might not typify the excitation of nonthermal activity by other central compact objects (such as the jets driven by black holes in AGN), underlines the need to advance observations of a larger number of plerions across the whole spectrum (especially of the younger, calorimetric systems), with the highest possible angular imaging and with sufficient temporal coverage to follow the variations of the fine scale structure which are so revealing of the compact object-surrounding world interaction marvelously exhibited by the Crab. It *does* behoove us theorists to turn some of the insights laboriously gleaned from the Crab into predictions for other plerions, especially the young ones with calorimetric morphology. I'm sure there will be plenty of surprises for all of us.

### Acknowledgements

I am particularly indebted to Jeff Hester for energetic discussions which clarified my understanding of the flow geometry around the Crab Pulsar, as well as many other entertaining aspects of astrophysics and of life, and to Anatoly Spitkovsky for illuminating collaboration and discussion. The research described here has been supported by NSF grant AST 9528271 and by NASA grant NAG 5-3073, and in part by the generosity of California's taxpayers.

### References

- Alsop, D., and Arons, J. 1988, *Phys. Fluids*, **31**, 839  
Arons, J. 1979, *Space Sci. Rev.*, **24**, 437  
Arons, J., and Tavani, M. 1993, *Astrophys. J.* **403**, 249  
Barnes, A., and Scargle, J.D. 1973 *Astrophys. J.* **184**, 251  
Bednarek, W., and Protheroe, R.J. 1997, *Phys. Rev. Lett.* **79**, 2616  
Begelman 1998a, *Astrophys. J.* **493**, 291  
Begelman 1998b, *Astrophys. J.*, submitted  
Bietenholz, M.F., and Kronberg, P.P. 1992, *Astrophys. J.* **393**, 206  
Bock, D. C.-J., Turtle, A.J., and Green, A.J. 1998, *Astron. J.*, in press (astro-ph/9807125)  
Chedia, O., Lominadze, J., Machabeli, G. *et al.* 1997, *Astrophys. J.* **479**, 313  
Coroniti 1990, F.V. 1990, *Astrophys. J.* **349**, 538  
de Jager, O.C., and Harding, A.K. 1992, *Astrophys. J.* **396**, 161  
de Jager, O.C., Harding, A.K., Michelson, P.F. *et al.* 1996 *Astrophys. J.* **457**, 253  
Gallant, Y.A., Hoshino, M., Langdon, A.B., *et al.* 1992, *Astrophys. J.* **391**, 73  
Gallant, Y.A., and Arons, J. 1994, *Astrophys. J.* **435**, 230  
Harrus, I.M., Hughes, J.P., and Helfand, D.J. 1996, *Astrophys. J. Lett.* **464**, L161  
Helfand, D.J., Becker, R.H., and White, R.L. 1994, *Astrophys. J.* **453**, 741

- Hester, J.J., Scowen, P.A., Sankrit, R., *et al.* 1995, *Astrophys. J.* **448**, 240
- Hoshino, M. and Arons, J. 1991, *Phys. Fluids B*, **3**, 818
- Hoshino, M. Arons, J., Gallant, Y. A., and Langdon, A.B. 1992, *Astrophys. J.* **390**, 454
- Hoshino, M. 1998, in *Neutron Stars and Pulsars: Thirty Years after the Discovery*, N. Shibazaki, N. Kawai, S. Shibata and T. Kifune, eds. (Tokyo: Univesal Academu Press), 491
- Kennel, C.F., and Coroniti, F.V. 1984a, *Astrophys. J.* **283**, 694; 1984b, *Astrophys. J.* **283**, 710
- Lampland, C.O. 1921, *Publ. Astr. Soc. Pacific* **33**, 79
- Langdon, A.B., Arons, J. and Max, C.E. 1988, *Phys. Rev. Lett.* **61**, 779
- Lyne, A.G., and Manchester, R.N. 1988, *Mon. Not. R. Astr. Soc.* **234**, 477
- Melatos and Melrose, A., and Melrose, D.B. 1996, *Mon. Not. R. Astr. Soc.* **279**, 1168
- Michel, F.C. 1994, *Astrophys. J.* **431**, 397
- Pelling, M., Paciesas, W.S., Peterson, L.E. *et al.* 1987 *Astrophys. J.* **319**, 416
- Rees and Gunn, M.J., and Gunn, J.E. 1974, *Mon. Not. R. Astr. Soc.* **167**, 1
- Romani, R.W. 1996, *Astrophys. J.* **470**, 469
- Sankrit, R., and Hester, J.J. 1997, *Astrophys. J.* **491**, 796
- Scargle, J.D. 1969, *Astrophys. J.* **156**, 401
- Tademaru, E. 1973, *Astrophys. J.* **183**, 625
- Tanvir, N.R., Thomson, R.C., and Tsikarishvili, E.G. 1997, *New Astron.*, **1**, 311
- van den Bergh, S., and Pritchett, C. 1989, *Astrophys. J. Lett.* **338**, L69
- Woltjer, L. 1958, *Bull. Ast. Inst. Netherlands*, **14**, 38